

PHYSICAL AND SPECTROSCOPIC CHARACTERISATION OF SAMARIUM
DOPED MAGNESIUM TELLURITE GLASS EMBEDDED SILVER
NANOPARTICLES

NURULHUDA BINTI MOHAMMAD YUSOFF

A thesis submitted in fulfilment of the
requirements for the award of the degree of
Doctor of Philosophy (Physics)

Faculty of Science
Universiti Teknologi Malaysia

AUGUST 2015

To my beloved father (Mohammad Yusoff bin Ismail) and
mother (Wan Pah binti Wan Mahmud),
to my dearest older sister (Fadilah binti Zaini),
to my valued sibling (Nurul Suhaila, Nurul Aini,
Mohammad Nasaruddin, Nurul Asmira,
Mohammad Nazrie, Nurul Nadia,
Mohammad Yusrie and Mohammad Iman).
There is nothing in my life that makes me happier and
cheerful than your love and care.

ACKNOWLEDGEMENTS

Alhamdulillah, all praise to ALLAH S.W.T, the Almighty, the All Merciful and the All Compassionate for giving me the strength, courage and patience to complete this project.

In preparing this thesis, I was in contact with academicians and researchers. They have contributed towards my understanding and thoughts. In particular, I wish to express my sincere appreciation to my thesis supervisor, Professor Dr. Md. Rahim Sahar for encouragement, guidance, critics and friendship. I am also very thankful to Assoc. Prof. Dr. Sib Krishna Ghoshal and Dr. Ramli for their guidance, advices and motivation. Without their continued support and interest, this thesis would not have been the same as presented here.

I am also indebted to Ministry of Education, Malaysia and Universiti Teknologi Malaysia (UTM) for funding my Ph.D. study. Lab assistance at Faculty of Science and Faculty of Mechanical, UTM, Universiti Sains Malaysia and Universiti Kebangsaan Malaysia also deserve special thanks for their assistance during the experiment.

I would like to show gratitude to my seniors, Dr. Raja Junaid Amjad, Dr. Reza Dousti, Dr. Asmahani, Dr. Fakhra Nawaz for the advice and helpful discussion contributing to my project. My fellow postgraduate students should also be recognised for their support, so my sincere appreciation extends to Siti Amlah, Ezza Syuhada, Puzi Anigrahawati, Amanina, Khamisah, Syarifah Fahsuhaizam, Siti Fatimah, Nur Aina Najihah, Siti Maisarah, Aina Mardhiah, Zahra Ashur and others who have provided assistance for my research project. Their views and tips are useful indeed. I am grateful to all my family members.

ABSTRACT

Three series of samarium doped magnesium tellurite glasses embedded with silver nanoparticles (Ag NPs) of composition $(89-x)\text{TeO}_2-10\text{MgO}-1\text{Sm}_2\text{O}_3-x\text{AgCl}$ with $0 \leq x \leq 1.0$ mol%, $(89.6-x)\text{TeO}_2-10\text{MgO}-(x)\text{Sm}_2\text{O}_3-0.4\text{AgCl}$ with $0.2 \leq x \leq 1.2$ mol% and $88.6\text{TeO}_2-10\text{MgO}-(x)\text{Sm}_2\text{O}_3-(1.4-x)\text{AgCl}$ with $0.2 \leq x \leq 1.0$ mol% were prepared using melt quenching technique. It is found that the glass samples are yellowish in colour depending on their compositions. The existence of broad hump in X-ray diffraction (XRD) pattern verifies the amorphous nature of glasses and the presence of silver nanoparticles with average diameter of 16.94 nm in the glass matrix is confirmed by transmission electron microscope (TEM) image. The glass density (ρ), molar volume (V_m) and ionic packing density (V_i) are in the range of $(4.91-5.51) \text{ g cm}^{-3}$, $(27.13-30.46) \text{ cm}^3 \text{ mol}^{-1}$ and $(0.444-0.498)$, respectively. The samples exhibit glass stability up to 102°C which indicates the enhancement in ability of glass formation. The fourier transform infrared (FTIR) and Raman spectra reveal modification in network structures which is evident from the shifted vibrational wave-number of TeO_4 and TeO_3 structural units located around 600 cm^{-1} and 700 cm^{-1} , respectively. Two surface plasmon resonance (SPR) peaks are detected at 550 nm for transverse oscillation and 578 nm for longitudinal oscillation from ultraviolet-visible (UV-Vis) absorption spectra. The optical energy band gap and Urbach energy are found in the range of $(2.81-3.13) \text{ eV}$ and $(0.18-0.26) \text{ eV}$, respectively. Refractive index and electronic polarisability have also been calculated and found in the range of $(2.35-2.45)$ and $(6.68-7.51) \text{ \AA}^3$, respectively. The absorption measurement is complemented with determination of bonding characteristic of Sm^{3+} and ligand via calculations of nephelauxetic ratio and Racah parameters. It is found that the addition of Sm^{3+} and Ag^0 alters the electron distribution which leads to the increase of the covalent bond between Sm and ligand. The glass samples are excited under 554 nm excitation wavelength and the emission spectra are found to consist of a single emission band corresponding to ${}^4\text{G}_{5/2} \rightarrow {}^6\text{H}_{11/2}$ transition. The intensity enhancement of such transition rises up to 3 times compare to glass without Ag NPs which is attributed to the local field effect and energy transfer from Ag^0 to Sm^{3+} . The quality factor, Q is also obtained in the range of 19.20-24.25 which is due to the phonon loss during the non-radiative emission. Meanwhile, decay half-life is determined in the range of $(1.4405-1.4459) \mu\text{s}$ depending on composition. The properties of this glass are very much dependent on the concentration of Sm^{3+} and Ag NPs. This type of glass has a wide potential to be used as red laser medium and in various photonic applications.

ABSTRAK

Tiga siri kaca magnesium tellurite berdopkan samarium oksida yang tertanam zarah nano perak (Ag NPs) dengan komposisi $(89-x)\text{TeO}_2-10\text{MgO}-1\text{Sm}_2\text{O}_3-x\text{AgCl}$ ($0 \leq x \leq 1.0$ mol%), $(89.6-x)\text{TeO}_2-10\text{MgO}-(x)\text{Sm}_2\text{O}_3-0.4\text{AgCl}$ ($0.2 \leq x \leq 1.2$ mol%) dan $88.6\text{TeO}_2-10\text{MgO}-(x)\text{Sm}_2\text{O}_3-(1.4-x)\text{AgCl}$ ($0.2 \leq x \leq 1.0$ mol%) disediakan melalui teknik pelindapan leburan. Kaca tersebut berwarna kekuningan bergantung kepada komposisinya. Kewujudan puncak yang lebar daripada corak pembelauan sinar-X (XRD) mengesahkan sifat amorfus kaca dan kehadiran zarah nano perak dengan purata diameter 16.94 nm di dalam matrik kaca disahkan melalui imej mikroskop elektron transmisi (TEM). Ketumpatan kaca (ρ), isipadu molar (V_m) dan ketumpatan padatan ionik (V_i) masing-masing dalam julat $(4.91-5.51) \text{ g cm}^{-3}$, $(27.13-30.46) \text{ cm}^3 \text{ mol}^{-1}$ dan $(0.444-0.498)$. Sampel tersebut mempamerkan kestabilan kaca sehingga 102°C yang menunjukkan peningkatan dalam keupayaan membentuk kaca. Spektrum transformasi fourier infra merah (FTIR) dan Raman menunjukkan pengubahsuaian dalam struktur rangkaian dan dibuktikan melalui anjakan getaran nombor gelombang bagi struktur unit TeO_4 dan TeO_3 yang masing-masing terletak di sekitar 600 cm^{-1} dan 700 cm^{-1} . Dua puncak resonans plasmon permukaan (SPR) dikesan pada 550 nm untuk ayunan melintang dan 578 nm untuk ayunan membujur daripada spektrum penyerapan ultra lembayung-boleh nampak (UV-Vis). Jurang tenaga optik dan tenaga Urbach ditemui masing-masing dalam julat $(2.81-3.13) \text{ eV}$ dan $(0.18-0.26) \text{ eV}$. Indeks biasan dan pengutuban elektronik juga telah dikira dan didapati masing-masing berada dalam julat $(2.35-2.45)$ dan $(6.68-7.51) \text{ \AA}^3$. Pengukuran penyerapan dilengkapi dengan pengiraan ciri ikatan antara Sm^{3+} dan ligan melalui kiraan nisbah nephelauxetic dan parameter Racah. Penambahan ion Sm^{3+} dan Ag^0 ditemui mengubah taburan elektron yang membawa kepada meningkatnya ikatan kovalen antara Sm dan ligan. Sampel kaca diuja pada panjang gelombang 554 nm dan spektrum pancaran didapati terdiri daripada jalur puncak tunggal mewakili transisi ${}^4\text{G}_{5/2} \rightarrow {}^6\text{H}_{11/2}$. Peningkatan keamatan pancaran transisi tersebut meningkat 3 kali ganda berbanding dengan kaca tanpa Ag NPs yang disebabkan oleh kesan medan setempat dan pemindahan tenaga daripada Ag^0 ke Sm^{3+} . Faktor kualiti, Q juga diperolehi dalam julat 19.20-24.25 yang disebabkan oleh kehilangan fonon semasa berlakunya pancaran tak radiatif. Sementara itu, setengah hayat pereputan juga telah ditentukan dalam julat $(1.4405-1.4459) \mu\text{s}$ bergantung kepada komposisi. Sifat kaca sangat bergantung kepada kepekatan Sm^{3+} dan Ag NPs. Kaca jenis ini mempunyai potensi yang luas untuk digunakan sebagai medium laser merah dan dalam pelbagai aplikasi fotonik.

TABLE OF CONTENTS

CHAPTER	TITLE	PAGE
	DECLARATION	ii
	DEDICATION	iii
	ACKNOWLEDGEMENTS	iv
	ABSTRACT	v
	ABSTRAK	vi
	CONTENTS	vii
	LIST OF TABLES	xi
	LIST OF FIGURES	xiv
	LIST OF SYMBOLS	xxiv
	LIST OF ABBREVIATIONS	xxvi
	LIST OF APPENDICES	xxvii
1	INTRODUCTION	1
	1.0 Introduction	1
	1.1 Problem Statement	4
	1.2 Objectives	5
	1.3 Scope of Study	6
	1.4 Significant of Study	7
	1.5 Chapter Organisation	8

2	LITERATURE REVIEW	9
2.0	Introduction	9
2.1	Background of Study	9
2.2	Plasmonic and Surface Plasmon Resonance (SPR)	13
2.3	Structural Morphology	
2.3.1	X-ray Diffraction	17
2.3.2	Transmission Electron Microscopy and High Resolution Transmission Electron Microscopy	21
2.4	Physical Properties	26
2.4.1	Density, Molar Volume, Ionic Packing Density	26
2.5	Thermal Parameter	28
2.5.1	Differential Thermal Analysis	28
2.6	Structural Properties	31
2.6.1	Fourier Transform Infrared Spectroscopy	31
2.6.2	Raman Spectroscopy	36
2.7	UV-Visible Spectroscopy	39
2.7.1	Absorption Coefficient	39
2.7.2	Optical Energy Band Gap	41
2.7.3	Urbach Energy	43
2.7.4	Refractive Index and Electronic Polarisability	45
2.7.5	Bonding Characteristic	48
	2.7.5.1 Nephelauxetic Ratio and Bonding Parameter	48
	2.8.5.2 Racah Parameter	50
2.8	Photoluminescence Spectroscopy	51
	2.8.1 Emission Process	51
	2.8.2 Energy Transfer	55
	2.8.3 Quality Factor	56
	2.8.4 PL Decay Lifetime	57

3	METHODOLOGY	60
3.0	Introduction	60
3.1	Glass Preparation	60
3.2	X-ray Diffraction (XRD)	64
3.3	Transmission Electron Microscopy (TEM)	65
3.4	Density	67
3.5	Energy Dispersive Analysis of X-ray (EDAX)	67
3.6	Differential Thermal Analysis (DTA)	68
3.7	Fourier Transform Infrared Spectroscopy (FTIR)	70
3.8	Raman Spectroscopy	71
3.9	UV-Vis Spectroscopy	72
3.10	Photoluminescence Spectroscopy	74
4	RESULT AND DISCUSSION	77
4.0	Introduction	77
4.1	Glass Formation	77
4.2	Structural Morphology	81
4.2.1	X-ray Diffraction	81
4.2.2	Transmission Electron Microscopy and High Resolution Transmission Electron Microscopy	83
4.2.3	Energy Dispersive Analysis of X-ray	86
4.3	Physical Properties	87
4.3.1	Density	87
4.3.2	Molar Volume	91
4.3.3	Ionic Packing Density	94
4.4	Thermal Parameter	97
4.4.1	Differential Thermal Analysis	97
4.5	Structural properties	100
4.5.1	Fourier Transform Infrared Spectroscopy	100
4.5.2	Raman Spectroscopy	105

4.6	UV-Visible Spectroscopy	112
4.6.1	Plasmon Absorption Spectrum	112
4.6.2	Absorption Spectra	114
4.6.3	Absorption Edge	116
4.6.4	Optical Energy Band Gap	120
4.6.5	Urbach Energy	126
4.6.6	Refractive Index	131
4.6.7	Electronic Polarisability	135
4.6.8	Bonding Characteristics	138
4.6.8.1	Nephelauxetic Ratio, β and Bonding Parameter, δ	138
4.6.8.2	Racah Parameter	143
4.7	Photoluminescence Spectroscopy	152
5	CONCLUSION AND RECOMMENDATION	164
5.0	Introduction	164
5.1	Conclusion	164
5.2	Recommendation	167
	REFERENCES	169
	Appendices A-H	189-206

LIST OF TABLES

TABLE NO.	TITLE	PAGE
2.1	The intense peak at 2θ of XRD pattern, hkl, lattice spacing and lattice constant of silver nanoparticles	20
2.2	The glass density, molar volume, ionic packing density of various tellurite glass systems	28
2.3	The glass transition temperature (T_g), Onset crystallisation temperature (T_x)/ crystallisation temperature (T_c), Thermal stability (T_x-T_g/T_c-T_g) and melting temperature (T_m) of various tellurite glass systems	30
2.4	Type of molecular vibration in IR (IR active or IR inactive). The type of vibration for Raman spectroscopy is also inserted	33
2.5	Peak position (in cm^{-1}) in FTIR spectra for various tellurite glass systems	35
2.6	Raman band assignment (in cm^{-1}) of various tellurite glass systems	39
2.7	Indirect optical band gap of various tellurite glasses systems	43

2.8	Urbach energy, ΔE of various tellurite glass systems	45
2.9	Refractive index (n), electronic polarisability (α_m) and metallization parameter (M) of various samarium doped tellurite glass systems	48
2.10	The value of $\bar{\beta}$ and δ of various tellurite glass systems	50
2.11	Excitation and emission wavelength of Sm^{3+} for different tellurite glass system	54
4.1	Nominal composition of magnesium tellurite glass system	79
4.2	Ratio of Sm^{3+} to Ag NPs in Series 3 glass system	79
4.3	EDAX result of S1-S5 glass samples	86
4.4	Actual composition of $(89-x)\text{TeO}_2-10\text{MgO}-1\text{Sm}_2\text{O}_3-x\text{AgCl}$ glass system	87
4.5	Density (ρ), Molar Volume (V_m), and Ionic Packing Density (V_t) of magnesium tellurite glass system. The calculation of ρ , V_m and V_t are shown in Appendix C	88
4.6	The value for T_g , T_x , T_x-T_g and T_m for magnesium tellurite glass system	98
4.7	IR absorption peak (in cm^{-1}) of magnesium tellurite glass system	105
4.8	Raman band assignment of magnesium tellurite glass system	107
4.9	The comparison of cut-off wavelength ($\lambda_{cut-off}$) between present glasses and other tellurite glasses systems	118

4.10	Indirect optical energy band gap of magnesium tellurite glass system	124
4.11	Urbach energy of magnesium tellurite glass system	128
4.12	Refractive index, molar refraction, electronic polarisability and metallization parameter of magnesium tellurite glass system	133
4.13	Average of nephelauxetic ratio, $\bar{\beta}$ and bonding parameter, δ of magnesium tellurite glass system	139
4.14	Comparison of average nephelauxetic ratio, $\bar{\beta}$ and bonding parameter, δ with different glasses hosts	143
4.15	Comparison of ligand field parameters and nephelauxetic function of magnesium tellurite glass system and other glasses hosts	145
4.16	Peak wavelength (λ_{em}) peak intensity (I_{em}), integrated intensity (I_i), full width at half maxima (FWHM) and decay half lifetime (τ) of magnesium tellurite glass system	155

LIST OF FIGURES

FIGURES NO.	TITLE	PAGE
1.1	The TeO ₄ tbp structural unit of tellurium oxide	3
2.1	Model for the formation of metallic silver nanoparticles	12
2.2	The oscillation of electron conduction band of nanoparticles	13
2.3	SPR peak of nanoparticles for spherical shape	14
2.4	SPR peak at 522 nm for tellurite glass containing 1.0 mol% heat treated Ag NPs	15
2.5	SPR band for different concentration of AgCl nanoparticles	16
2.6	SPR peaks of Ag NPs in 0.5 mol% (A05H8) and 1.0 mol% (A10H8) Ag NPs in tellurite glass	17
2.7	The schematic of Bragg law	18
2.8	XRD pattern of Sm ³⁺ co-doped Yb ³⁺ in sodium tellurite glass showing a broad hump	19
2.9	XRD pattern of Ag NPs in Soda-lime glass matrix	20

2.10	XRD pattern of growth Ag NPs at different heat treatment time in tellurite glass	21
2.11	The black spot of TEM shows Ag NPs	22
2.12	Normal distribution (Bell curve shape) shows the average (mean) at the centre of the bell	23
2.13	(a) Aggregated and non-spherical Ag NPs (b) Gaussian distribution of Ag NPs	24
2.14	(a) Ag NPs image (b) Gaussian distribution (c) HRTEM image of lattice constant of Ag NPs	24
2.15	(a) TEM image of $58\text{P}_2\text{O}_5\text{--}40\text{MgO--}1.5\text{AgCl--}0.5\text{Er}_2\text{O}_3$ Inset shows a selected area of electron diffraction pattern (SAED) of the glass. (b) Gaussian distribution with 37 nm average diameter size of Ag NPs (c) lattice spacing of Ag NPs at (200) plane detected by High Resolution Transmission Electron Microscope	25
2.16	(a) TEM image of Ag NPs in $74.5\text{TeO}_2\text{--}25\text{ZnO--}0.5\text{Eu}_2\text{O}_3$ with 0.3 mol% AgCl (b) Gaussian distribution with average diameter size is ~8nm (c) lattice spacing of (200) direction	25
2.17	Typical DTA curves of zinc tellurite glass	29
2.18	FTIR spectra of tellurite glass of Er^{3+} doped sodium tellurite glasses	34
2.19	Three lines of scattered light by a molecule. Stokes line appears more intense than anti-Stokes line	36
2.20	Polarisation of incident light of an isotropic molecule is scattered at an angle θ_s (scattered angle)	37

2.21	A typical Raman spectra of Er ³⁺ doped zinc tellurite glasses	38
2.22	Light absorption phenomenon in a sample with a thickness of d	40
2.23	Three regions of absorption coefficient versus photon energy	41
2.24	Tauc plot of indirect optical band gap $(\alpha h\nu)^{1/2}$ and direct optical band gap $(\alpha h\nu)^2$ versus photon energy, $h\nu$ of TeO ₂ -TiO ₂ -Nd ₂ O ₃ -WO ₃ glass system	42
2.25	Direct (E_{opt}^D) and indirect optical energy band gap (E_{opt}^I). Note that, direct gap occur at $k = 0$, while indirect gap occur at $k \neq 0$	42
2.26	Urbach tails of localized states in the band gap	44
2.27	Absorption and emission processes	52
2.28	Excitation and emission process in PL	53
2.29	Energy level of 1.0 mol% Sm ₂ O ₃ doped Niobium Borotellurite glass at 401 nm excitation wavelength	54
2.30	Energy transfer from NPs to RE ion in (a) Down conversion emission (b) Up-conversion emission. R and NR are denoted as radiative and non-radiative, respectively	55
2.31	A schematic energy diagram of Sm ³⁺ /Yb ³⁺ : Ag tri-doped tellurite glass	56
2.32	Typical radiative decay curve of half-life	58
2.33	Decay profile of ⁴ G _{5/2} → ⁶ H _{7/2} transition for Sm ³⁺ ion doped TZKC glass system	59

2.34	Decay curve of 1.0 mol% Sm ₂ O ₃ doped TMZNB, TCZNB and TSZNB glass for ⁴ G _{5/2} → ⁶ H _{7/2} transition	59
3.1	Flow of sample preparation	62
3.2	The schematic diagram of sample preparation. Note: the cooling rate after the furnace is switch off is arbitrary	63
3.3	Schematic diagram of X-ray diffractometer	65
3.4	Schematic diagram of transmission electron microscope showing the areas in which the electron is going through	66
3.5	EDAX schematic diagram	68
3.6	Schematic diagram of differential thermal analyser	69
3.7	Fourier Transform Infrared instrument setup	71
3.8	The setup of Raman spectrometer	72
3.9	A schematic diagram of UV-Vis spectroscopy	74
3.10	Schematic diagram of Photoluminescence experimental setup	75
4.1	Glass samples of (a) Series 1 (b) Series 2 (c) Series 3 and (d) glass without Sm ₂ O ₃	80
4.2	Typical X-ray diffraction patterns of (89-x)TeO ₂ -10MgO-1Sm ₂ O ₃ -xAgCl glass system	82
4.3	Typical X-ray diffraction patterns of (89.6-x)TeO ₂ -10MgO-xSm ₂ O ₃ -0.4AgCl glass system	82

4.4	Typical X-ray diffraction patterns of 88.6TeO ₂ -10MgO-xSm ₂ O ₃ -(1.4-x)AgCl glass system	83
4.5	(a) TEM image of Ag NPs in S3 (b) Gaussian Distribution of Ag NPs particles size of S3	84
4.6	(a) Fast Fourier Transformation image of Ag NPs (b) d-spacing of Ag NPs at (111) plane	85
4.7	A plot of density versus Ag NPs concentration	89
4.8	A plot of density versus Sm ₂ O ₃ concentration	90
4.9	A plot of density versus Sm ³⁺ : Ag NPs	90
4.10	Molar volume versus Ag NPs concentration	92
4.11	Molar volume versus Sm ₂ O ₃ concentration	93
4.12	Molar volume versus Sm ³⁺ : Ag NPs	93
4.13	Ionic packing density, V _t versus Ag NPs concentration	95
4.14	Ionic packing density, V _t versus Sm ₂ O ₃ concentration	96
4.15	Ionic packing density, V _t versus Sm ³⁺ : Ag NPs	96
4.16	A typical DTA curve for S1 of Series 1 glass system	97
4.17	Thermal parameter T _x , T _g and T _x -T _g versus Ag NPs concentration	99
4.18	Thermal parameter T _x , T _g and T _x -T _g versus Sm ₂ O ₃ concentration	99

4.19	Thermal parameter T_x , T_g and T_x-T_g versus Sm^{3+} : Ag NPs	100
4.20	(a) IR spectra of $(89-x)TeO_2-10MgO-1Sm_2O_3-xAgCl$ glass system (b) TeO_4 tbp group versus Ag NPs concentration	102
4.21	IR spectra of $(89.6-x)TeO_2-10MgO-xSm_2O_3-0.4AgCl$ glass system	103
4.22	IR spectra of $88.6TeO_2-10MgO-xSm_2O_3-(1.4-x)AgCl$ glass system	104
4.23	Raman spectra of $(89-x)TeO_2-10MgO-1Sm_2O_3-xAgCl$ glass system	106
4.24	Raman spectra of $(89.6-x)TeO_2-10MgO-xSm_2O_3-0.4AgCl$ glass system	106
4.25	Raman spectra of $88.6TeO_2-10MgO-xSm_2O_3-(1.4-x)AgCl$ glass system	107
4.26	The wavenumber of TeO_4 tbp and TeO_3 tp vibrations versus Ag NPs concentration	110
4.27	Intensity of Boson peak versus Ag NPs concentration	111
4.28	The wavenumber of TeO_4 tbp and TeO_3 tp versus Sm_2O_3 concentration	111
4.29	The wavenumber of TeO_4 tbp and TeO_3 tp versus Sm^{3+} : Ag NPs	112
4.30	The absorption spectrum of glass without Sm^{3+} ion for S0. There are two SPR bands, a transverse SPR located at 550 nm, and a longitudinal SPR located at 578 nm	113

4.31	The absorption spectra of (89-x)TeO ₂ -10MgO-1Sm ₂ O ₃ -xAgCl glass system	114
4.32	The absorption spectra of (89.6-x)TeO ₂ -10MgO-xSm ₂ O ₃ -0.4AgCl glass system	115
4.33	The absorption spectra of 88.6TeO ₂ -10MgO-xSm ₂ O ₃ -(1.4-x)AgCl glass system	115
4.34	Cut-off wavelength, $\lambda_{cut-off}$ versus Ag NPs concentration	119
4.35	Cut-off wavelength, $\lambda_{cut-off}$ versus Sm ₂ O ₃ concentration	119
4.36	Cut-off wavelength, $\lambda_{cut-off}$ versus Sm ³⁺ :Ag NPs	120
4.37	Tauc plot of indirect optical energy band gap of (89-x)TeO ₂ -10MgO-1Sm ₂ O ₃ -xAgCl glass system	121
4.38	Tauc plot of indirect optical energy band gap of (89.6-x)TeO ₂ -10MgO-xSm ₂ O ₃ -0.4AgCl glass system	121
4.39	Tauc plot of indirect optical energy band gap of 88.6TeO ₂ -10MgO-xSm ₂ O ₃ -(1.4-x)AgCl glass system	122
4.40	Indirect optical energy band gap, E_{opt}^I versus Ag NPs concentration	124
4.41	Indirect optical energy band gap, E_{opt}^I versus Sm ₂ O ₃ concentration	125
4.42	Indirect optical energy band gap, E_{opt}^I versus Sm ³⁺ : Ag NPs	125

4.43	ln (α) versus hv of (89-x)TeO ₂ -10MgO-1Sm ₂ O ₃ -xAgCl glass system	126
4.44	ln (α) versus hv of (89.6-x)TeO ₂ -10MgO-xSm ₂ O ₃ -0.4AgCl glass system	127
4.45	ln (α) versus hv of 88.6TeO ₂ -10MgO-xSm ₂ O ₃ -(1.4-x)AgCl glass system	127
4.46	Urbach energy versus Ag NPs concentration	129
4.47	Urbach energy versus Sm ₂ O ₃ concentration	130
4.48	Urbach energy versus Sm ³⁺ : Ag NPs	130
4.49	Refractive index, n versus Ag NPs concentration	133
4.50	Refractive index, n versus Sm ₂ O ₃ concentration	134
4.51	Refractive index, n versus Sm ³⁺ : Ag NPs	134
4.52	Variation of electronic polarizability, α_m versus Ag NPs concentration	137
4.53	Variation of electronic polarizability, α_m versus Sm ₂ O ₃ concentration	137
4.54	Variation of electronic polarizability, α_m versus Sm ³⁺ : Ag NPs	138
4.55	Bonding parameter, δ versus Ag NPs concentration	141
4.56	Bonding parameter, δ versus Sm ₂ O ₃ concentration	142
4.57	Bonding parameter, δ versus Sm ³⁺ : Ag NPs	142

4.58	Plot of B and C Racah parameters versus Ag NPs concentration	146
4.59	Plot of Dq/B ratio versus Ag NPs concentration	146
4.60	Plot of nephelauxetic function, h versus Ag NPs concentration	147
4.61	Plot of B and C Racah parameters versus Sm ₂ O ₃ concentration	148
4.62	Plot of Dq/B ratio versus Sm ₂ O ₃ concentration	149
4.63	Plot of nephelauxetic function, h versus Sm ₂ O ₃ concentration	149
4.64	Plot of B and C Racah parameters versus Sm ³⁺ : Ag NPs	150
4.65	Plot of Dq/B ratio versus Sm ³⁺ : Ag NPs	151
4.66	Plot of nephelauxetic function, h versus Sm ³⁺ : Ag NPs	151
4.67	The visible down conversion luminescence spectra of (89-x)TeO ₂ -10MgO-1Sm ₂ O ₃ -xAgCl glass system	154
4.68	The visible down conversion luminescence spectra of (89.6-x)TeO ₂ -10MgO-xSm ₂ O ₃ -0.4AgCl glass system	154
4.69	The visible down conversion luminescence spectra of 88.6TeO ₂ -10MgO-xSm ₂ O ₃ -(1.4-x)AgCl glass system	155
4.70	PL integrated intensity versus Ag NPs concentration	156
4.71	PL integrated intensity versus Sm ₂ O ₃ concentration	156
4.72	PL integrated intensity versus Sm ³⁺ : Ag NPs	157
4.73	Partial energy diagram of magnesium tellurite glass system	158

4.74	Plot of Quality factor versus Ag NPs concentration	159
4.75	Plot of Quality factor versus Sm ₂ O ₃ concentration	159
4.76	Plot of Quality factor versus Sm ³⁺ : Ag NPs	160
4.77	Normalised number of photons versus a decay time for S1	161
4.78	Decay half-life versus Ag NPs concentration	162
4.79	Decay half-life versus Sm ₂ O ₃ concentration	162
4.80	Decay half-life versus Sm ³⁺ : Ag NPs	163

LIST OF SYMBOLS

\bar{x}	-	arithmetic mean
ρ	-	glass density
V_m	-	molar volume
V_t	-	ionic packing density
V_i	-	packing density parameter
T_g	-	transition glass temperature
T_c	-	crystallisation temperature
T_x	-	onset crystallization temperature
T_m	-	melting temperature
ΔT	-	thermal stability
ν	-	vibrational frequency
μ	-	reduced mass
I	-	intensity of transmitted light
α	-	absorption coefficient
E_{opt}	-	optical energy band gap
ΔE	-	Urbach energy
$h\nu$	-	photon energy
n	-	refractive index

F	-	field strength
R_m	-	molar refraction
M	-	metallization parameter
α_m	-	electronic polarisability
β	-	nephelauxetic ratio
δ	-	bonding parameter
$\bar{\beta}$	-	average nephelauxetic ratio
h	-	nephelauxetic function
k_{ion}	-	central metal ion
τ	-	half-life
Q	-	quality factor

LIST OF ABBREVIATIONS

ASTM	-	American Society for Testing and Materials
TMO	-	transition metal oxide
tbp	-	trigonal bipyramidal
tp	-	trigonal pyramidal
O _{eq}	-	equatorial oxygens
O _{ax}	-	axial oxygens
ZnO	-	Zinc oxide
MgO	-	Magnesium oxide
RE	-	Rare earth
BO	-	Bridging oxygens
NBO	-	Non-bridging oxygens
NPs	-	Nanoparticles
SPR	-	Surface plasmon resonance
ET	-	Energy transfer
CCD	-	charge couple device

LIST OF APPENDICES

APPENDIX NO.	TITLE	PAGE
A	Full width at half maxima	189
B	Batch calculation	190
C	Density, molar volume, ionic packing density	192
D	EDAX spectrum	196
E	Calculation of Racah parameter	199
F	Calculation of Quality factor	202
G	Plot of decay curve	203
H	List of publications	206

CHAPTER 1

INTRODUCTION

1.0 Introduction

Glass can be define as an amorphous solid which is stand for absences of long-range order or structureless solid. There is no regularity in the arrangement of its molecular constituent. Morey [1] defines glass as an inorganic substance in which its behaviour is analogous to the liquid state of that substance. According to American Society for Testing and Materials (ASTM), glass is defined as an inorganic product of fusion which has cooled to a rigid condition without crystallizing. Meanwhile, Secrist and Mackenzie [2] define a glass as a non-crystalline solid. The historical of glass definitions obviously refers and reflects to the evolution of glass development regarding to the technological interest and commercially important. Glasses are easily produced from a melt by rapid cooling to a sufficiently low temperature which is well known as melt quenching technique. The fast cooling rate generally in the order of 10^7 degrees per second may avoid the crystallisation to occur in the glassy phase. Of course, there are many other technique for preparing glass [3]. However, the melt quenching technique has been used in this study since it is the cheapest and the shortest time consuming. Glasses can be fabricated into a variety of shapes and sizes with an appropriate composition [4]. Glass features are essentially depending on its composition [5].

The number of materials to form glasses is rapidly increases [6]. Among the most motivated studies of glassy materials, tellurite based glasses draw much interest because of their unique properties such as high dielectric constant and excellent transmission in the visible as well as IR wavelength regions, good mechanical strength and chemical durability [7-10]. These glasses also possess higher refractive index which is approximately in the range of 2.0 to 2.5 [11-14] and their low melting temperature (about 800°C) contributes to the high possibility of stable glass forming using a conventional melt quenching method [10]. Although, pure tellurium oxide cannot form glass by itself but needs another element known as glass modifier such as alkali metal, alkaline earth metal oxide and transition metal oxide (TMO) to improve the network connectivity then produce a stable tellurite glass [15-16] with increasing non-bridging oxygen [15]. Thus, reduce the rigidity of TeO₂ structure and easily produce disorder structure. TeO₂ glassy and crystalline states are built by coordination of Te⁴⁺ ions in TeO₄ groups as trigonal bipyramidal (tbp) form with bridging oxygen [17]. In TeO₄ tbp linkage, two oxygen atoms are located in the axial site, while the other two and the lone electron pair of tellurium are located in the three equatorial sites. Kim [18] acknowledged that the equatorial Te-O bonds are slightly shorter than the axial bonds. Damas et al. [19] reported that the two equatorial oxygens (O_{eq}) possessed a distance of 1.9Å from the Te atom, while the two axial oxygens (O_{ax}) possesses a distance of 2.1Å from Te atom. Trigonal bipyramids are linked by each other by sharing their vertices which form a continuous three-dimensional structure [20] as shown in Figure 1.1. The basic structure of TeO₂ glass network often changes from TeO₄ to TeO₃₊₁ and/or TeO₃ in the presence of network modifier. The substitution of network modifier such as MgO and ZnO would produce the stable tellurite glass [21-22]. The addition of such modifiers would modify and increase non-bridging oxygen, consequently open up the glass structure. In this case, the Te-O-Te linkages in TeO₄ will break into TeO₃₊₁ or TeO₃ structural unit. In addition, it is reported that the alkaline earth metals are good network modifiers for tellurite glass [23-24].

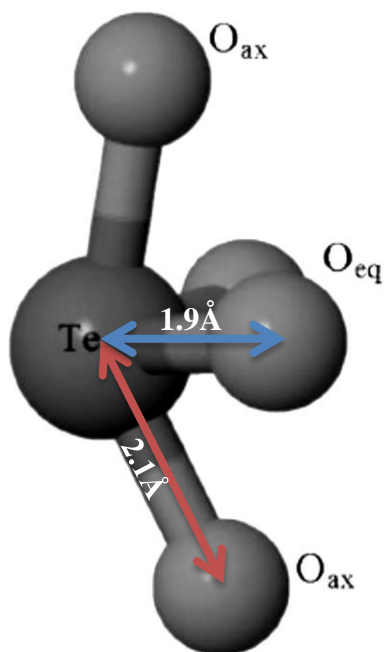


Figure 1.1: The TeO_4 tbp structural unit of tellurium oxide. The distances of Te-O bond are also shown [19].

Te-O bonds can also be easily broken and accommodate heavy metal oxides or rare earth (RE) precisely called as dopant. Nelson et al. [25] have proposed two important effects of dopant ions in terms of their local environment. Firstly, each of the dopant ions can occupy an individual site which is determined by the configuration of the structural unit in the melt. Secondly, dopant can modify the spatial geometry of the nearby glass network to outfit their own bonding requirement. Moreover, dopants can also act as network modifiers and thus promote the formation of high number of non-bridging oxygen (NBO) [26]. TeO_2 based glass is good for hosting rare earth ion since they provide low phonon energy (~ 750 nm), which minimizes non-radiative losses [27-28]. RE doped glass has long held tradition of facilitating lasing character inside the glass matrix. Samarium is one of the important active ion in rare earth family which exhibits strong orange-red luminescence in the visible region and very useful in high density optical storage, under water communication, colour displays and visible solid state lasers. The luminescence properties either down or up conversion phenomena has widely been

studied in various based glass. These studies show that the emission intensities are strongly dependent of Sm^{3+} concentration and glass composition [29].

It is worth to notice that RE doped glasses may exhibit some unwanted effects such as concentration quenching due to the energy-transfer to neighbouring ions. So in order to enhance the luminescence efficiency and remove this drawback, several methods can be adopted. The embedding of metallic nanoparticles (NPs) inside the glass host thus changing the environment felt by the RE ions is introduced a successful strategy [30-34]. Recently, Sm^{3+} ion is verified as a dopant while Au or Ag NPs are demonstrated as stimulating agents for the enhancements of absorption and emission properties [35]. The metallic NPs assisted strong modifications in the rare earth transition probabilities caused by local field effect and energy transfer are easily detected from emission measurements. The composition, shape and size of NPs play significant roles towards their interaction with external radiation [36].

1.1 Problem Statement

The nano era revolution demands the synthesis of new nanostructured materials, if possible by a simple technique but with remarkable properties and versatile applications [37]. Previous study of nanoglass has been focused on embedding of metallic nanoparticles in glass containing rare earth ions only [36, 38-41]. In order to pursue this area, a well-designed new glass composition should be developed and presented. Rare doped tellurite glass embedded nanoparticles has been reported to improve luminescence intensity due to energy transfer and local field effect [36, 38-41]. The enhancement of luminescence intensity and the avoidance of quenching effect is a challenge effort. Up to date, most of study focused on the embedment of Au NPs in $\text{Er}^{3+}/\text{Yb}^{3+}$ co-doped tellurite glass [42], Er^{3+} doped tellurite glass [43], meanwhile the embedment of Ag NPs on Er^{3+} doped tellurite glass [40], Dy^{3+} doped tellurite glass [41], $\text{Sm}^{3+}:\text{Yb}^{3+}$ co-doped tellurite glass [37]. In sequence,

the embedment of Ag NPs with an optimum concentration into tellurite glass containing single rare earth especially Sm^{3+} is important to be emphasized. Additionally, since there is a lack of report on these glasses, it is of particular important to study these glasses in order to give more information on the influence of Ag NPs and Sm^{3+} ion on the glass. It is therefore, the aim of this work to characterise the glass by means of their physical, thermal, structural, absorption features and the quality of the emission intensity.

1.2 Objectives

In order to solve the problem as stated in Section 1.1, several objectives have been outlined as follows,

- 1) To prepare glass samples containing Ag NPs and Sm^{3+} ion by melt quenching technique in three glass series of composition,
 - a. Series 1: $(89-x)\text{TeO}_2-10\text{MgO}-1\text{Sm}_2\text{O}_3-x\text{AgCl}$, where $0 \leq x \leq 1.0$ in mol%
 - b. Series 2: $(89.6-x)\text{TeO}_2-10\text{MgO}-x\text{Sm}_2\text{O}_3-0.4\text{AgCl}$ where $0.2 \leq x \leq 1.2$ in mol%
 - c. Series 3: $88.6\text{TeO}_2-10\text{MgO}-x\text{Sm}_2\text{O}_3-(1.4-x)\text{AgCl}$ where $0.2 \leq x \leq 1.0$ in mol%.
- 2) To determine the influence of substituted Ag NPs and Sm^{3+} ion in the glass on physical and thermal properties by calculating density, molar volume, ionic packing density and thermal parameters, respectively.

- 3) To investigate the role of Ag NPs and Sm^{3+} ion on structural properties of the glass by measuring the change of band position in Infrared and Raman spectroscopy.
- 4) To investigate the role of Ag NPs and Sm^{3+} ion on the absorption features of the glass by measuring optical energy band gap, Urbach energy, refractive index, and electronic polarizability up to bonding parameter accomplished from UV-Visible spectroscopy.
- 5) To explore the effect of Ag NPs and Sm^{3+} ion on luminescence enhancement or quenching effect, spectroscopic quality factor and decay half lifetime of the glass accomplished from Photoluminescence Spectroscopy.

1.3 Scope of Study

This study attempted to identify the characteristic of bulk glass samples in three different compositions prepared by a conventional melt quenching technique. The glass densities are measured by Archimedes method since the glass samples have an irregular shape. The measured densities are very useful to determine the molar volume and ionic packing density. Thermal parameters such as glass transition temperature (T_g), onset crystallisation temperature (T_x) and melting temperature (T_m) are also determined by thermogram curve obtained from Differential Thermal Analyser (DTA). In term of structural modification, the research will focus on the change of band position in Infrared spectra and Raman spectra obtained from IR spectrometer and Raman spectrometer, respectively. In this respect, the discussion will only be focus on the change of wavenumber for TeO_4 trigonal bipyramidal, TeO_{3+1} tetrahedral and TeO_3 trigonal pyramidal. Meanwhile, the study on the absorption feature obtained from UV-Vis spectrophotometer will covers optical

energy band gap, Urbach energy, refractive index and electronic polarizability up to calculation of Racah parameters of bonding characteristic only. Then the enhancement factor, quality factor and decay lifetime will be accomplished from Photoluminescence spectrometer.

1.4 Significant of Study

Study of metallic silver nanoparticles substituted at TeO₂ host site provides useful information on the advancement of the glass knowledge. By knowing the amplitude of enhancement factor of luminescence characteristic, the effectiveness of Ag NPs will become clearer. This study also will contribute to a better understanding on bonding and structural characteristic in order to get an optimum amount of Ag NPs which could explain the enhancement phenomena in luminescence. Furthermore, the fundamental phenomenon on the optical characteristic is no exception to be discussed in this study. According to this, the relationship between optical characteristic, glass structural modification and luminescence enhancement can be well explained. This research is very important in view that the required level of luminescence intensity of samarium ion for multipurpose of usage and very significant in the development of nanoscience. Moreover, the optimize method for controlling the Ag NPs and Sm³⁺ ions in improving the structural and optical characteristics of magnesium tellurite glasses may constitute a basis for their large scale synthesis useful for sundry of applications.

1.5 Thesis organisation

This thesis is made up by five main chapters namely introduction, literature review, methodology, results and discussions, and conclusion and recommendation. In the Chapter 1 (Introduction), a briefly explanation about tellurite glass, problem statement, objective, scope of study, significant of study and thesis organisation are provided. In Chapter 2 (Literature review), the basic theoretical of physical, thermal, structural, absorption and luminescence related to the previous research works are described. In Chapter 3 (Methodology), the glass preparation, method of measurement for each characterisation and principle work of each instrument as well as the characterisation framework are provided. In Chapter 4 (Results and Discussions), the obtained data are analysed by plotting graphs and presenting in table. The analysed data well discussed by comparing to the previous results in past research works. In Chapter 5 (Conclusion and Recommendation), the finding are concluded and summarised. Some recommendations for future works toward the prepared glass sample are listed.

REFERENCES

- [1] Morey, G. W. *The Properties of Glass*. 1th. ed. New York: Reinhold Publishing Corporation. 1938
- [2] Secrist, D. R., Mackenzie, J. D. *Modern Aspects of the Vitreous State*. London: Butterworths. 1960
- [3] Uhlmann, D.R., Yinnon, H. (1983). *The Formation of Glasses*. In Uhlmann, D. R., Kreidl, N. J. *Glass: Science and Technology*. (pp. 1-47). New York: Academic Press
- [4] Pye, L. D., Stevens, H. J., and La Course, W. C. *Introduction to Glass Science*, Plenum Press, New York. 1972
- [5] Sokolov, V.O., Plotnichenko, V. G., Koltashev, V.V. (2009) Structure of Barium Chloride-oxide Tellurite Glasses. *Journal of Non-crystalline Solids*. 355: 1574-1584
- [6] Klinger, M. I. (1988). Glassy Disordered Systems: Topology, Atomic Dynamics and Localized Electron States. *Physics Reports*. 165 (5-6): 275 – 397
- [7] Rivera, V. A. G., Osorio, S. P. A., Manzani, D., Messaddeq, Y., Nunes, L. A. O., and Marega Jr. (2011). Growth of Silver Nano-particle embedded in Tellurite Glass: Interaction between Localized Surface Plasmon Resonance and Er^{3+} ions. *Optical Materials* 33: 888-892
- [8] El-Mallawany, R.A.H. *Tellurite Glasses Handbook: Physical Properties and Data*. New York: CRC Press. 2002
- [9] Jha, A., Richards, B., Jose, G., Fernandez, T. T., Joshi, P., Jiang, X., and Lousteau, J. (2012). Rare-earth Ion doped TeO_2 and GeO_2 Glasses as Laser Materials, *Progress in Materials Science*. 57: 1426-1491

- [10] Babu, P., Seo, H. J., Kesavulu, C. R., Jang, K. H., Jayasankar, C. K. (2009). Thermal and Optical Properties of Er^{3+} - doped Oxyfluorotellurite Glasses. *Journal of Luminescence*. 129: 444-448
- [11] Pavani, P. G., Suresh, S., Mouli, V. C. (2011). Studies on Boro Cadmium Tellurite Glasses. *Optical Materials*. 34: 215-220
- [12] Sakida, S., Nanba, T., and Miura, Y. (2006). Refractive-index Profiles and Propagation Losses of Er^{3+} -doped Tungsten Tellurite Glass Waveguide by Ag^+ - Na^+ ion-exchange. *Materials Letters*. 60: 3413-3415
- [13] Pavani, P. G., Sadhana, K., and Mouli, V. C. (2011). Optical, Physical and Structural Studies of Boro-Zinc Tellurite Glasses. *Physica B*. 406:1242-1247
- [14] Yousef, E., Hotzel, M., and Russel, C. (2004). Linear and Non-Linear Refractive Indices of Tellurite Glasses in the System TeO_2 - WO_3 - ZnF_2 . *Journal of Non-Crystalline Solids*. 342: 82-88
- [15] Rajendran, V., Palanivelu, N., Chaudhuri, B.K., Goswami, K. (2003). Characterisation of Semiconducting V_2O_5 - Bi_2O_3 - TeO_2 Glasses through Ultrasonic Measurements. *Journal of Non-Crystalline Solids*. 320: 195-209
- [16] Moraes, J. C. S., Nardi, J. A., Sidel, S. M., Mantovani, B. G., Yukimitu, K., Reynoso, V. C. S., Malmonge, L. F., Ghofraniha, N., Ruocco, G., Andrade, L. H. C., Lima, S. M. (2010). Relation among Optical, Thermal and Thermo-optical Properties and Niobium Concentration in Tellurite Glasses, *Journal of Non-Crystalline Solids*. 356: 2146-2150
- [17] Dimitrov, V., J. (1987). Phase Diagram and IR Spectral Investigations of the $2\text{TeO}_2 \cdot \text{V}_2\text{O}_5$ - $\text{Li}_2\text{O} \cdot \text{V}_2\text{O}_5 \cdot 2\text{TeO}_2$ System. *Journal of Solid State Chemistry*. 66: 256-262
- [18] Kim, S.H., Yoko, T. (1995). Nonlinear Optical Properties of TeO_2 -based Glasses: MO_x - TeO_2 (M = Sc, Ti, V, Nb, Mo, Ta, and W) Binary Glasses. *J. American Ceramic Society*. 78 (4): 1061-1065
- [19] Damas, P., Coelho, J., Hungerford, G., Hussain, N.S. (2012). Structural Studies of Lithium Boro Tellurite Glasses doped with Praseodymium and Samarium Oxides. *Materials Research Bulletin*. 47: 3489 - 3494

- [20] Zhou, Y., Yang, Y., Huang, F., Ren, J., Yuan, S., Chen, G. (2014). Characterization of New Tellurite Glasses and Crystalline Phases in the $\text{TeO}_2\text{-PbO-Bi}_2\text{O}_3\text{-B}_2\text{O}_3$ System, *Journal of Non-Crystalline Solids*. 386: 90–94
- [21] Terny, S. De la Rubia, M.A. Alonso, R. E. de Frutos, J. Frechero, M.A. (2015). Structure and Electrical Behavior Relationship of a Magnesium–Tellurite Glass using Raman and Impedance Spectroscopy. *Journal of Non-Crystalline Solids*. 411: 13–18
- [22] Kozhukharov, V. Bürger, H. Neov, S. and Sidzhimov, B. (1986). Atomic Arrangement of a Zinc-Tellurite Glass. *Polyhedron*. 5 (3): 771–777
- [23] Sekiya, T., Mochida, N., Ohtsuka, A. (1994). Raman Spectra of MO-TeO_2 ($\text{M} = \text{Mg, Sr, Ba and Zn}$) Glasses. *Journal of Non-Crystalline Solids*. 168: 106-114
- [24] Sekiya, T., Mochida, N., Ohtsuka, A. (1992). Raman spectra of $\text{MO}_{1/2}\text{-TeO}_2$ ($\text{M} = \text{Li, Na, K, Rb, Cs and Tl}$) Glasses, *Journal of Non-Crystalline Solids*. 144: 128-144
- [25] Nelson, C., Furukawa, I., Nelson, W.B. (1983). Transition metal ions in glasses: Network modifiers or quasi-molecular complexes?. *Materials Research Bulletin*. 18: 959-966
- [26] Turkey, G., and Dawy, M. (2002). Spectral and Electrical Properties of Ternary ($\text{TeO}_2\text{-V}_2\text{O}_5\text{-Sm}_2\text{O}_3$) Glasses, *Materials Chemistry and Physics*. 77: 48–59
- [27] Ozdanova, J. Ticha, H. Tichy, L. (2010). Raman Studies and some Physical Properties of Selected $(\text{PbO})_x(\text{Nb}_2\text{O}_5)_y(\text{TeO}_2)_{1-x-y}$ Glasses, *Optical Materials*. 32: 950-955
- [28] Jlassi, I. Elhouichet, H. Ferid, M. Chtourou, R. Oueslati, M. (2010). Effect of Heat Treatment on the Structural and Optical Properties of Tellurite Glasses doped Erbium. *Optical Materials*. 32: 743-747
- [29] Sundari, S. S. Marimuthu, K. Sivaraman, M. Babu, S. S. (2010). Composition Dependent Structural and Optical Properties of Sm^{3+} doped Sodium Borate and Sodium Fluoroborate Glasses. *Journal of Luminescence*. 130: 1313-1319

- [30] Maier, S.A. Atwater, H.A. (2005). Plasmonics: Localization and Guiding of Electromagnetic Energy in Metal/Dielectric Structures. *Journal of Applied Physics*. 98: 011101
- [31] Barnes, W.L. Dereux, A. and Ebbesen, T.W. (2003). Surface Plasmon Subwavelength Optics. *Nature*. 424: 824-830
- [32] Le, F. Brandl, D.W. Urzhumov, Y.A. Wang, H. Kundu, J. Halas, N.J. Aizpurua, J. Nordlander, P. (2008). Metallic Nanoparticle Arrays: A Common Substrate for Both Surface-Enhanced Raman Scattering and Surface-Enhanced Infrared Absorption. *ACS Nano*. 2:707-718
- [33] Lal, S. Link, S. Halas, N.J. (2007). Nano-optics from Sensing to Waveguiding, *Nature Photonics*. 1: 641-648
- [34] Geddes, C.D. Lakowicz, J. R. (2002). Metal-Enhanced Fluorescence, *Journal of Fluorescence*. 12:121-129
- [35] Du, Y. Y. Chen, B. J. Pun, E. Y. B. Wang, Z. Q. Zhau, X. Lin, H. (2015). Silver Nanoparticles Enhanced Multichannel Transition Luminescence of Pr^{3+} in Heavy Metal Germanium Tellurite Glasses. *Optic Communications*. 334: 203-207
- [36] Rivera, V.A.G., Ledemi, Y. Osorio, S.P.A. Manzani, D., Messaddeq, Y., Nunes, L.A.O., and Jr, E.A. (2012). Efficient plasmonic coupling between Er^{3+} : (Ag/Au) in tellurite glasses. *Journal of Non-crystalline Solids*. 358 (2): 399-405
- [37] Dousti, M.R., Amjad, R.J., Hosseinian, R.S., Salehi, M., Sahar, M.R. (2015). Photoluminescence Study of Sm^{3+} - Yb^{3+} co-doped Tellurite Glass embedding Silver Nanoparticles. *Journal of Luminescence*. 159: 100-104
- [38] Som, T., Karmakar, B. (2011). Synthesis and enhanced photoluminescence in novel $\text{Au}_{\text{core}}\text{Au}-\text{Ag}_{\text{shell}}$ nanoparticles embedded Nd^{3+} -doped antimony oxide glass hybrid nanocomposites. *Journal of Quantitative Spectroscopy & Radiative Transfer*. 112: 2469–2479
- [39] Som, T., Basudeb, K. (2009). Nano Au enhanced upconversion in dichroic Nd^{3+} :Au-antimony glass nanocomposites. *Solid State Sciences*. 11: 1044–1051

- [40] Dousti, M.R., Sahar, M.R., Amjad, R.J., Ghoshal, S.K., Awang, A. (2013). Surface enhanced Raman scattering and up-conversion emission by silver nanoparticles in erbium–zinc–tellurite glass. *Journal of Luminescence*. 143: 368–373
- [41] Dousti, M.R., Hosseinian, S.R. (2014). Enhanced upconversion emission of Dy³⁺-doped tellurite glass by heat-treated silver nanoparticles. *Journal of Luminescence*. 154: 218–223
- [42] Kassab, L.R.P., Camilo, M.E., Amancio, C.T., da Silva, D.M., Martinelli, J.R. (2011). Effects of gold nanoparticles in the green and red emissions of TeO₂–PbO–GeO₂ glasses doped with Er³⁺–Yb³⁺. *Optical Materials*. 33: 1948–1951
- [43] Awang, A., Ghoshal, S.K., Sahar, M.R., Dousti, M.R., Amjad, R.J., Nawaz, F. (2013). Enhanced Spectroscopy Properties and Judd-Ofelt Parameters of Er-doped Tellurite Glass: Effect of Gold Nanoparticles. *Current Applied Physics* 13: 1813-1818
- [44] Srivastava, P., Rai, S. B., Rai, D. K. (2004). Effect of Lead Oxide on Optical Properties of Pr³⁺ doped Some Borate based Glasses. *Journal of Alloys and Compounds*. 368: 1-7
- [45] Coelho, J., Freire, C., Hussain, N. S. (2012). Structural Studies of Lead Lithium Borate Glasses doped with Silver Oxide. *Spectrochimica Acta Part A*. 86: 392-398
- [46] Maheshvaran, K., Linganna, K. and Marimuthu, K. (2011). Composition Dependent Structural and Optical Properties of Sm³⁺ doped Boro-Tellurite Glasses. *Journal of Luminescence*. 131 (12): 2746-2753
- [47] Babu, A. M., Jamalaih, B. C., Sasikala, T., Saleem, S. A., Moorthy, L. M. (2011). Absorption and Emission Spectral Studies of Sm³⁺ doped Lead Tungstate Tellurite Glasses. *Journal of Alloys and Compounds*. 509 (14): 4743-4747
- [48] Ravi, O., Reddy, C. M., Manoj, L. and Raju, B. D. P. (2012). Structural and Optical Studies of Sm³⁺ ions doped Niobium Borotellurite Glasses. *Journal of Molecular Structure*. 1029: 53-59
- [49] Venkatramu, V., Babu, P., Jayasankar, C. K., Troster, Th., Sievers, W., Wortmann, G. (2007). Optical Spectroscopy of Sm³⁺ ions in Phosphate and Fluorophosphate Glasses. *Optical Materials*. 29: 1429–1439

- [50] Mahato, K. K., Rai, D. K., Rai, S. B. (1998). Optical Studies of Sm³⁺ doped Oxyfluoroborate Glass. *Solid State Communications*. 108: 671-676
- [51] Mahraz, Z.A.S., Sahar, M.R., Ghoshal, S.K., Dousti, M.R. (2013). Concentration Dependent Luminescence Quenching of Er³⁺ doped Zinc Boro-Tellurite Glass. *Journal of Luminescence* 144: 139-145
- [52] Jayasimhadri, M., Moorthy, L. R., Saleem, S. A., Ravikumar, R. V. S. S. N. (2006). Spectroscopic Characteristics of Sm³⁺-doped Alkali Fluorophosphates Glasses. *Spectrochimica Acta A*. 64: 939-944
- [53] Dominiak-Dzik, G. (2005). Sm³⁺ doped LiNBO₃ Crystal, Optical Properties and Emission Cross Sections. *Journal of Alloys and Compounds*. 391: 26-32
- [54] Sudhakar, K. S. V., Reddy, M. S., Rao, L. S., Veeraiyah, N. (2008). Influence of Modifier Oxide on Spectroscopic and Thermoluminescence Characteristics of Sm³⁺ ion in Antimony Borate Glass System. *Journal of Luminescence*. 128: 1791
- [55] Filho, A. G. S., Filho, J. M., Melo, F. E. A., Custodio, M. C. C., Lebullenger, R., Hernandez, A. C. (2000). Optical Properties of Sm³⁺ doped Lead Fluoroborate Glasses. *Journal of Physics and Chemistry of Solids*. 61: 1535-1542
- [56] Jamalaiah, B. C., Kumar, J. S., Babu, A. M., Suhasini, T., Moorthy, L. R. (2009). Photoluminescence Properties of Sm³⁺ in LBTAf Glasses. *Journal of Luminescence*. 129: 363
- [57] Amjad, R. J., Dousti, M. R., Sahar, M. R., Shaukat, S. F., Ghoshal, S. K., Sazali, E. S., Nawaz, F. (2014). Silver Nanoparticles Enhanced Luminescence of Eu³⁺ -doped Tellurite Glass. *Journal of Luminescence*. 154: 316-321
- [58] Reisfeld, R., Pietraszkiewicz, M., Saraidarov, T., Levchenko, V., (2009). Luminescence Intensification of Lanthanide Complexes by Silver Nanoparticles Incorporated in Sol-gel Matrix. *Journal of Rare Earth*. 27: 544-549
- [59] Malta, O. L., dos Santos, M. A. C. (1990). Theoretical Analysis of the Fluorescence Yield of Rare Earth ions in Glasses Containing Small Metallic Particles. *Chemical Physics Letters*. 174: 13-18

- [60] Hayakawa, T., Selvan, S. T. and Nogami, M. (1999). Field Enhancement Effect of Small Ag Particles on the Fluorescence from Eu^{3+} -doped SiO_2 Glass. *Applied Physics Letters*. 74: 1513-1515
- [61] Giehl, J. M., Pontuschka, W. M., Barbosa, L. C., Chilloce, E. F., Da Costa, Z. M., Alves, S. (2011). Thermal Precipitation of Silver Nanoparticles and Thermoluminescence in Tellurite Glasses. *Optical Materials*. 33: 1884–1891
- [62] Som, T., Karmakar, B. (2009). Enhancement of Er^{3+} Upconverted Luminescence in Er^{3+} : Au-Antimony Glass Dichroic Nanocomposites Containing Hexagonal Au Nanoparticles. *Journal of the Optical Society of America B*. 26: B21-B27
- [63] Brown M. D, Suteewong, T. Kumar. R. S. S, D’Innocenzo, V. Petrozza, A. Lee, M. M. Wiesner, U. Snaith, H. J. (2011). Plasmonic Dye-Sensitized Solar Cells using Core–Shell Metal–Insulator Nanoparticles. *Nano Letters*. 11:438–45
- [64] Tokonami, S., Yamamoto, Y., Shiigi, H., Nagaoka, T. (2012). Synthesis and Bioanalytical Applications of Specific-Shaped Metallic Nanostructures: A Review. *Analytica Chimica Acta*. 716: 76-91
- [65] Kreibig, U. Vollmer, M. *Optical Properties of Metal Clusters*. New York: Springer Verlag. 1995
- [66] Qi, J., Xu, T., Wu, Y., Shen, X., Dai, S., Xu, Y. (2013). Ag Nanoparticles Enhanced Near-IR Emission from Er^{3+} ions doped Glasses. *Optical Materials*. 35: 2502-2506
- [67] Tsung, C. -K., Kou, X. S., Shi, Q. H., Zhang, J. P., Yeung, M. H., Wang, J. F., Stucky, G. D. (2006). Selective Shortening of Single-Crystalline Gold Nanorods by Mild Oxidation. *Journal of the American Chemical Society*. 128: 5352-5353
- [68] Cullity, B. D. *Element of X-Ray Diffraction*. 2nd. ed. Massachusetts: Addison-Wesley Publishing Company. 1978
- [69] Nawaz, F., Sahar, M. R., Ghoshal, S. K., Awang, A., Amjad, R. J. (2014). Judd–Ofelt Analysis of Spectroscopic Properties of Sm^{3+} doped Sodium Tellurite Glasses co-doped with Yb^{3+} . *Journal of Luminescence*. 147: 90–96.

- [70] Theivasanthi, T. and Alagar, M. (2012). Electrolytic Synthesis and Characterizations of Silver Nanopowder. *Nano Biomedicine Engineering*. 4 (2): 58-65
- [71] Veron, O., Blondeau, J. –P., Meneses, D. D. S. and Vignolle, C. A. (2013). Characterization of Silver or Copper Nanoparticles embedded in Soda-lime Glass after a Staining Process. *Surface and Coatings Technology*. 227: 48-57
- [72] Dousti, M.R. (2014). Plasmonic Effect of Silver Nanoparticles on the Upconversion Emissions of Sm³⁺-doped Sodium-Borosilicate Glass. *Measurement*. 56: 117-120
- [73] Davis, S. A. *Electron Microscopy: Colloid Science: Theory, Methods and Applications*. 2005
- [74] Williams, D. B. Carter, C. B. *Transmission Electron Microscopy: A Textbook for Materials Science*. New York: Springer. 2009
- [75] Das, R., Nath, S. S., Chakdar, D., Gope, G., Bhattacharjee, R. (2009). Preparation of Silver Nanoparticles and Their Characterization, *Open Access Rewards System*. DOI : 10.2240/azojono0129
- [76] Jillavenkatesa, A., Dapkunas, S. J. and Lum Lin-Sien, H. *Particle size characterization*. NIST Recommended Practical Guide. 2001
- [77] Allen, T. *Particle Size Measurement*. 5th. ed. Chapman and Hall. 1997
- [78] *ASM Handbook. Powder Metal Technology and Applications*. ASM International. 1998
- [79] *Engineered Materials Handbook: Ceramic and Glasses*. ASM International. 1991
- [80] Dousti, M.R., Sahar, M.R., Ghoshal, S.K., Amjad, R.J., Ariffin, R. (2012). Up-conversion Enhancement in Er³⁺-Ag co-doped Zinc Tellurite Glass: Effect of Heat Treatment. *Journal of Non-Crystalline Solids*. 358: 2939-2942.
- [81] Amjad, R. J., Sahar, M. R., Ghoshal, S. K., Dousti, M. R., Riaz, S. Tahir, B. A. (2012). Enhanced Infrared to Visible Upconversion Emission in Er³⁺ doped Phosphate Glass: Role of Silver Nanoparticles. *Journal of Luminescence*. 132: 2714-2718

- [82] Yiannopoulos, Y. D., Varsamis, C. P. E., Kamitsos, E. I. (2001). Density of Alkali Germanate Glasses related to Structure. *Journal of Non-crystalline Solids*. 293-295: 244-249
- [83] Jen, J.S. and Kalinowski (1989). An Esca Study of the Bridging To Non-Bridging Oxygen Ratio in Sodium Silicate Glass and the Correlations to Glass Density and Refractive Index. *Journal of Non-crystalline Solids*. 38 & 39: 21-26
- [84] Shelby, J. E. *Introduction to Glass Science and Technology*. 2nd. ed. London: Royal Society of Chemistry. 2005
- [85] El-Diasty, F., Wahab, A. A. (2006). Optical Band Gap Studies on Lithium Aluminum Silicate Glasses doped with Cr³⁺ ions. *Journal of Applied Physics*. 100: 093511-1-7
- [86] Sanad, A. M., Moustafa, A. G., Moustafa, F. A. and El-Mongy, A. A. (1985). Role of Halogens on the Molar Volume of Some Glasses Containing Vanadium. *Central Glass and Ceramic Research Institute Bulletin*. 32 (3): 53-56
- [87] Makishima, A., Mackenzie, J. D. (1973). Direct Calculation of Young's Modulus of Glass. *Journal of Non-crystalline Solids*. 12: 35-45
- [88] Saddeek, Y. B. (2004). Structural Analysis of Alkali Borate Glasses. *Physica B*. 344: 163-175
- [89] Ahmmad, S. K. Samee, M. A. Edukondalu, A. Rahman, S. (2012). Physical and Optical Properties of Zinc Arsenic Tellurite Glasses. *Results in Physics*. 2:175-181
- [90] Dousti, M.R., Sahar, M.R., Ghoshal, S.K., Amjad, R.J., Samavati, A.R. (2013). Effect of AgCl on Spectroscopic Properties of Erbium doped Zinc Tellurite Glass. *Journal of Molecular Structure*. 1035: 6 -12
- [91] Ghoshal, S.K., Zainuddin, A., Arifin, R., Sahar, M.R., Rohani, M.S., Hamzah, K. (2015). Samarium Concentration and Optical Correlation of Tellurite Glass. *Advanced Materials Research*. 1107: 443-448
- [92] Ghoshal, S.K., Zake, N.S.M., Arifin, R., Sahar, M.R., Rohani, M.S., Hamzah, K. (2015). Optical Properties of Oxy-Chloride Tellurite Glass: Role of Samarium ions. *Advanced Materials Research*. 1107: 437-442

- [93] Sazali, E.S., Sahar, M.R., Ghoshal, S.K., Arifin, R., Rohani, M.S., Amjad, R.J. (2015). Efficient Optical Enhancement of Er³⁺ doped Lead-Tellurite Glass embedded with Gold Nanoparticles: Role of Heat-Treatment. *Journal of Non-Crystalline Solids*. 410: 174-179
- [94] Fares, H., Jlassi, I., Elhouichet, H., Férid, M. (2014). Investigations of Thermal, Structural and Optical Properties of Tellurite Glass with WO₃ adding. *Journal of Non-Crystalline Solids*. 396–397: 1–7
- [95] Dousti, M.R., Ghassemi, P., Sahar, M.R., Mahraz, Z.A.(2014). Chemical Durability and Thermal Stability of Er³⁺ doped Zinc Tellurite Glass containing Silver Nanoparticles. *Chalcogenide Letters*. 11 (3): 111-119
- [96] Ersundu, A. E., Karaduman, G., Celikbilek, M., Solak, N., Aydin, S. (2010). Effect of Rare-earth Dopants in the Thermal Behaviour of Tungsten-Tellurite Glasses. *Journal of Alloys and Compounds*. 508: 266-272
- [97] Sahar, M. R., Jehbu, A. K., Karim, M. M. (1997). TeO₂-ZnO- ZnCl₂ Glasses for IR Transmission. *Journal of Non-Crystalline Solids*. 213 & 214: 164-167
- [98] Wang, F., Chen, B.J., Lin, H., Pun, E.Y.B. (2014). Spectroscopic Properties and External Quantum Yield of Sm³⁺ doped Germanotellurite Glasses. *Journal of Quantitative Spectroscopy & Radiative Transfer*. 147: 63-70
- [99] Zuraini, C., Yusoff, W.M.D.W., Halimah, M.K. and Zaidan, A.W. (2011). Dielectric Properties of B₂O₃-TeO₂-Sm₂O₃ Glasses System. *Solid State Science and Technology*. 19 (2): 285-300
- [100] Wang, J.S., Vogel, E.M., Snitzer, E. (1994). Tellurite Glass: A new Candidate for Fiber Devices. *Optical Materials*: 187-203
- [101] Widanarto, W., Sahar, M.R., Ghoshal, S.K., Arifin, R., Rohani, M.S., Effendi, M. Thermal, Structural and Magnetic Properties of Zinc-Tellurite Glasses Containing Natural Ferrite Oxide. *Materials Letters* 108 (2013) 289–292
- [102] Simon, I. *Modern Aspects of the Vitreous state*. London: Butterworth. 1964
- [103] El-Deen, L. M. S., Al Salhi, M. S., Elkholy, M. M. (2008). IR and UV Spectral Studies for Rare Earths-doped Tellurite Glasses. *Journal of Alloys and Compounds*. 465: 333-339

- [104] Leng, Y. *Materials Characterization: Introduction to Microscopic and Spectroscopic Methods*. New Jersey: John Wiley & Sons. 2008
- [105] Awang, A., Ghoshal, S.K., Sahar, M.R., Arifin, R. (2015). Gold Nanoparticles Assisted Structural and Spectroscopic Modification in Er^{3+} , *Optical Materials*. 42: 495-505
- [106] Rada, S., Dan, V., Rada, M., Culea, E. (2010). Gadolinium-Environment in Borate–Tellurate Glass Ceramics Studied by FTIR and EPR Spectroscopy. *Journal of Non-Crystalline Solids*. 356: 474-479
- [107] Gowda, V. C. V., Reddy, C. N., Radha, K. C., Anavekar, R. V., Etourneau, J., Rao, K. J. (2007). Structural Investigations of Sodium Diborate Glasses Containing PbO , Bi_2O_3 and TeO_2 : Elastic Property Measurements and Spectroscopic Studies. *Journal of Non-Crystalline Solids*. 353: 1150-1163
- [108] Rada, S., Culea, M., Culea, E. (2008). Structure of TeO_2 - B_2O_3 Glasses Inferred from Infrared Spectroscopy and DFT Calculations. *Journal of Non-Crystalline Solids*. 354: 5491-5495
- [109] Nawaz, F., Sahar, M.R., Ghoshal, S.K., Awang, A., Ahmed, I. (2014). Concentration Dependent Structural and Spectroscopic Properties of $\text{Sm}^{3+}/\text{Yb}^{3+}$ co-doped Sodium Tellurite Glass. *Physica B*. 433: 89-95
- [110] Long, D. A. *Raman Spectroscopy*. New York: McGraw-Hill International Book Company. 1977
- [111] Laserna, J. J. *Modern Techniques in Raman Spectroscopy*. New York: John Wiley & Sons. 1996
- [112] Fuxi, G. *Optical and spectroscopic properties of glass*. Shanghai: Springer Verlag, Shanghai Scientific and Technical Publishers. 1992
- [113] Amer, M. S. *Raman Spectroscopy for Soft Matter Applications*. United State: John Wiley & Sons. 2009
- [114] Jlassi, I., Elhouichet, H., Hraiech, S. Ferid, M. (2012). Effect of Heat Treatment on the Structural and Optical Properties of Tellurite Glasses doped Erbium. *Journal of Luminescence*. 132: 832-840
- [115] Wang, G., Zhang, J., Dai, S., Yang, J., Jiang, Z. (2005). Thermal Analyses, Spectral Characterization and structural interpretation of Yb^{3+} doped TeO_2 - ZnO-ZnCl_2 Glasses. *Physics Letters A* 341 (2005) 285–290.

- [116] Suthanthirakumar, P., Karthikeyan, P., Manimozhi, P.K., Marimuthu, K. (2015). Structural and Spectroscopic Behavior of $\text{Er}^{3+}/\text{Yb}^{3+}$ co-doped Boro-tellurite Glasses. *Journal of Non-Crystalline Solids*. 410: 26-34
- [117] Tikhomirov, V. K., Jha, A., Perakis, A., Sarantopoulou, E., Naftaly, M., Krasteva, V., Li, R., Seddon, A. B. (1999). An Interpretation of the Boson Peak in Rare Earth Ion Doped Glasses. *Journal of Non-Crystalline Solid*. 256 & 257: 89-94
- [118] Yin, D., Qi, Y., Peng, S., Zheng, S., Chen, FF., Yang, G., Wang, X., Zhou, Y. (2014). $\text{Er}^{3+}/\text{Tm}^{3+}$ Codoped Tellurite Glass for Blue Upconversion—Structure, Thermal Stability and Spectroscopic Properties. *Journal of Luminescence*. 146: 141–149
- [119] Jaba, N., Mermet, A., Duval, E., Champagnon, B. (2005). Raman Spectroscopy Studied of Er^{3+} -doped Zinc Tellurite Glasses. *Journal of Non-Crystalline Solids*. 351: 833-837
- [120] Zheng, S., Zhou, Y., Yin, D., Xu, X., Wang, X. (2013). Influence of WO_3 on the Spectroscopic Properties and Thermal Stability of $\text{Er}^{3+}/\text{Ce}^{3+}$ codoped Tellurite Glasses. *Optical Materials*. 35: 1526-1531
- [121] Sreenivasulu, V., Upender, G., Swapna, Priya, V. V., Mouli, V. C., Prasad, M. (2014). Raman, DSC, ESR and Optical Properties of Lithium Cadmium Zinc Tellurite Glasses. *Physica B*. 454: 60–66
- [122] Khatir, S., Romain, F., Portier, J., Rossignol, S., Tanguy, B., Videau, J. J., Turrell, S. (1993). Raman Studies of Recrystallized Glasses in the Binary, TeO_2 - PbO System. *Journal of Molecular Structure*. 298:13
- [123] Knowles, A. and Burgess, C. *Practical Absorption Spectrometry*. New York: Chapman and Hall. 1984
- [124] Tauc, J. *Amorphous and Liquid Semiconductors*. London: Plenum. 1974
- [125] Mott, N. F. and Davis, E. A. (1970). *Philosophy Magazine*. 22: 903
- [126] Al-Ani, S. K. J. and Higazy, A. A. (1991). Study of Optical Absorption Edges in $\text{MgO-P}_2\text{O}_5$ Glasses. *Journal of Materials Science*. 26: 3670-3674
- [127] Chimalawong, P., Kaewkhao, J., Kedkaew, C. and Limsuwan, P. (2010). Optical and Electronic Polarizability Investigation of Nd^{3+} -doped Soda-lime Silicate Glasses. *Journal of Physics and Chemistry of Solids*. 71: 965-970

- [128] Abdel-Baki, M. and El-Diasty, F. (2006). Optical Properties of Oxide Glasses containing Transition Metals: Case of Titanium- and Chromium-containing Glasses. *Current Opinion in Solid State and Materials Science*. 10: 217-229
- [129] Eraiah, B. (2010). Optical Properties of Lead-Tellurite Glasses doped with Samarium Trioxide. *Bulletin of Materials Science*. 33: 391-394
- [130] Eraiah, B. (2006). Optical Properties of Samarium doped Zinc Tellurite Glasses. *Bulletin of Materials Science*. (4): 375-378
- [131] Urbach, F. (1953). *Physics Review*. 92: 1324
- [132] Choudhury, B., Dey, M., Choudury, A. (2013). Defect Generation, d-d Transition, and Band Gap Reduction in Cu-doped TiO₂ Nanoparticles. *International Nano Letters*. 3:25 doi: 10.1186/2228-5326-3-25
- [133] Moss, T.S. *Photoconductivity in the Elements*. New York: Academic Press Incorporation.1952
- [134] Reddy, R. R., Gopal, K. R., Narasimhulu, K., Reddy, L. S. S., Kumar, K. R., Reddy, C. V. K. Ahmed, S. N. (2008). Correlation Optical Electronegativity and Refractive Index of Semiconductors, Insulators, Oxides and Alkali Halides. *Optical Materials*. 31: 209
- [135] Dimitrov, V. and Sakka, S. (1996). Electronic Oxide Polarizability and Optical Basicity of Shape Oxides. 1. *Journal of Applied Physics*. 79 (3): 1736
- [136] Oo, H.M., Kamari, H-M., Yusoff, W.M.D.W. (2012). Optical Properties of Bismuth Tellurite based Glass. *International Journal of Molecular Sciences*. 13: 4623-4631
- [137] Dimitrov, V., Komatsu, T. (1999). Electronic polarizability, optical basicity and non-linear optical properties of oxide glasses. *Journal of Non-Crystalline Solids*. 249: 160-179
- [138] Lorentz, H. A. (1880). On the Relation between the Propagation Speed of Light and Density of a Body. *Annals of Physics*. 9: 641-665
- [139] Lorenz, L. (1880). About the Constant of Refraction. *Annals of Physics*. 11: 70-103
- [140] Jorgensen, C. K. *Modern Aspect of Ligand field Theory*. Amsterdam: North-Holland Publishing Co. 1971

- [141] Suchocki, A., Biernacki, S. W., Grinberg, M. (2007). Nephelauxetic Effect in High-Pressure Luminescence of Transition-Metal Ion Dopants. *Journal of Luminescence*. 125: 266-270
- [142] Carnall, W. T., Fields, P. R., Rajnak, K. (1968). Electronic Energy Levels in the Trivalent Lanthanide Aquo Ions. I. Pr^{3+} , Nd^{3+} , Pm^{3+} , Sm^{3+} , Dy^{3+} , Ho^{3+} , Er^{3+} , and Tm^{3+} . *The Journal of Chemical Physics*. 49 (10): 4424
- [143] Som, T., Karmakar, B. (2008). Infrared-to-red Upconversion Luminescence in Samarium-doped Antimony Glasses. *Journal of Luminescence*. 128: 1989–1996
- [144] Sinha, S. P. *Complexes of the Rare Earth*. Oxford: Pergamon Press. 1966
- [145] Sajna, M.S. Thomas, S. Mary, K.A.A. Joseph, C. Biju, P.R. Unnikrishnan, N.V., Spectroscopic Properties of Er^{3+} ions in Multicomponent Tellurite Glasses, *Journal of Luminescence* 159 (2015) 55-65
- [146] Selvaraju, K., Marimuthu, K. (2012). Structural and Spectroscopic Studies on Er^{3+} doped Boro-Tellurite Glasses. *Physica B*. 407: 1086-1093
- [147] Selvaraju, K., Marimuthu, K., Seshagiri, T.K., Godbole, S.V. (2011) Thermal, Structural and Spectroscopic Investigations on Eu^{3+} doped Boro-Tellurite Glasses. *Materials Chemistry and Physics*. 131: 204-210
- [148] Venkateswarlu, M., Mahamuda, Sk., Swapna, K., Prasad, M.V.V.K.S., Rao, A.S., Babu, A.M., Shakya, S., Prakash, G.V. (2015). Spectroscopic Studies of Nd^{3+} doped Lead Tungsten Tellurite Glasses for the NIR Emission at 1062 nm. *Optical Materials*. 39: 8-15
- [149] Maheshvaran, K., Marimuthu, K. (2012). Concentration Dependent Eu^{3+} doped Boro-Tellurite Glasses-Structural and Optical Investigations. *Journal of Luminescence*. 132: 2259-2267
- [150] Hassan, M. A., Farouk, M., Abdullah, A. H., Kashef, I., Elok. M. M. (2012). ESR and Ligand Field Theory Studies of Nd_2O_3 doped Boro-chromate Glasses. *Journal of Alloys and Compounds*. 539: 233-236
- [151] Ahmad, F. (2014). Study of Effect of Alkali/ Alkaline Earth Addition on the Environment of Boro-chromate Glasses by Means of Spectroscopic Analysis. *Journal of Alloys and Compounds*. 586: 605-610
- [152] Gao, F., Zhang, S. (1997). Investigation of Mechanism of Nephelauxetic Effect. *Journal of Physics and Chemistry of Solids*. 58 (12): 1991-1994

- [153] Seeber, W., Ehrt, D., Eberdoff-Heidepriem, D. (1994). Spectroscopic and Laser Properties of Ce^{3+} - Cr^{3+} - Nd^{3+} co-doped Fluoride Phosphate and Phosphate Glasses. *Journal of Non-Crystalline Solids*. 171: 94-104
- [154] Pal, P., Penhouet, T., D'Anna, V., Hagemann, H. (2013). Effect of Pressure on the Free Ion and Crystal Field Parameters of Sm^{2+} in BaFBr and SrFBr Hosts. *Journal of Luminescence*. 134: 678-685
- [155] Keester, K. L., White, W. B. *Crystal Field Spectra and Chemical Bonding in Manganese Minerals*, Paper and Proceedings of the fifth General Meeting. International Mineral Association. London: Cambridge. 1968
- [156] Henning, J. C. M. (1967). Covalency and Hyperfine Structure of 3d5 Ions in Crystal Fields. *Journal of Physics Letters A*. 24: 40
- [157] Ballhausen, C. J. *Introduction to Ligand Field Theory*, New York: McGraw-Hill Press. 1962
- [158] Lumb, M. D. *Luminescence spectroscopy*. London: Academic Press., 1978
- [159] Sasikala, T., Moorthy, L.R., Babu, A.M. (2013). Optical and Luminescent Properties of Sm^{3+} doped Tellurite Glasses. *Spectrochimica Acta Part A: Molecular and Biomolecular Spectroscopy*. 104: 445-450
- [160] Selvaraju, K., Marimuthu, K. (2013). Structural and Spectroscopic Studies on Concentration Dependent Sm^{3+} doped Boro-Tellurite Glasses. *Journal of Alloys and Compounds*. 553: 273-281
- [161] Auzel, F. (2004). Upconversion and Anti-Stokes Processes with f and d Ions in Solids. *Chemical Reviews*. 104: 139
- [162] Gamelin, D. R., Güdel, H-U. (2001). Upconversion Processes in Transition and Rare Earth Metal Systems. *Topics in Current Chemistry*. 214: 1-56
- [163] Pan, Z., Crosby, A., Obadina, O., Ueda, A., Aga, R. Mu, R., Morgan, S. H. (2010). Study of Tb-doped $\text{Li}_2\text{O-LaF}_3\text{-Al}_2\text{O}_3\text{-SiO}_2$ Glasses Containing Silver Nanoparticles. *MRS Sym.Proc.* 1028: 1208-O09-16
- [164] Som, T. Karmakar, B. (2009). Nanosilver Enhanced Upconversion Fluorescence of Erbium Ions in Er^{3+} : Ag-antimony Glass Nanocomposites. *Journal of Applied Physics*. 105: 013102
- [165] de Araujo, C. B., Kassab, L. R. P., Kobayashi, R. A., Naranjo, L. P. and Santa Cruz, P. A. (2006). Luminescence enhancement of Pb^{2+} ions in $\text{TeO}_2\text{-PbO-GeO}_2$ glasses containing silver nanostructures. *Journal of Applied Physics*. 99:123522

- [166] Marchi, S. D., Mattei, G., Mazzoldi, P., Sada, C. and Miotello, A. (2002). Two Stages in the Kinetics of Gold Cluster Growth in Ion-implanted Silica during Isothermal Annealing Inoxidizing Atmosphere. *Journal of Applied Physics*. 92: 4249-4254
- [167] Jimenez, J. A., Lysenko, S. and Liu, H. (2007). Enhanced UV-excited Luminescence of Europium ions in Silver/tin-doped Glass. *Journal of Luminescence*. 128: 831-833
- [168] Nurulhuda Binti Mohammad Yusoff (2011). *Optical Properties of Magnesium Phosphate Glass doped Samarium*. Master Degree, Universiti Teknologi Malaysia, Skudai
- [169] Rajesh, D., Naidu, M. D., Ratnakaram, Y. C. (2014). Synthesis and Photoluminescence Properties of $\text{NaPbB}_5\text{O}_9:\text{Dy}^{3+}$ Phosphor Materials for White Light Application. *Journal of Physics and Chemistry of Solids*. 75: 1210–1216
- [170] Hunter, E. E. *Practical Electron Microscopy: A Beginner's Illustrated Guide*. New York: Cambridge University Press. 1993
- [171] Wilson, M. Kannangara, K. Smith, G. Simmons, M. Raguse, B. *Nanotechnology: Basic Science and Emerging Technologies*. Florida: CRC Press. 2002
- [172] Vaughan, D. *Energy Dispersive X-Ray Microanalysis*, Middleton: NORAN Instrument. 1999
- [173] Wendlandt, W. W. *Thermal Analysis*. 3rd. ed. New York: Wiley-Interscience. 1986
- [174] Smith, B. C. *Fundamentals of Fourier Transform Infrared Spectroscopy*. Florida: CRC Press. 1996
- [175] Smith, W. Dent, G. *Introduction, Basic Theory, Principles and Resonance Raman Scattering. Modern Raman Spectroscopy*. England: John Wiley & Sons. 2005
- [176] Skoog, D. A. Holler, F. J. Crouch, S. R. *Principle of Instrumental Analysis*. 6th. ed. Thomson Brooks/Cole. 2006
- [177] Lakowicz, J. R. *Principles of Fluorescence Spectroscopy*. 3rd. ed. New York: Springer. 2006

- [178] Widanarto, W., Sahar, M.R., Ghoshal, S.K., Arifin, R., Rohani, M.S. Hamzah, K. (2013). Effect of Natural Fe₃O₄ Nanoparticles on Structural and Optical Properties of Er³⁺ doped tellurite Glass. *Journal of Magnetism and Magnetic Materials*. 326: 123-128
- [179] Dousti, M. R., Sahar, M. R., Amjad, R. J., Ghoshal, S. K., Khorramnazari, A., Basirabad, A. D., Samavati, A. (2012). Enhanced Frequency Upconversion in Er³⁺-doped Sodium Lead Tellurite Glass Containing Silver Nanoparticles. *The European Physical Journal D*. 66: 237
- [180] Lide, D. R. *CRC Handbook of Chemistry and Physics*. 86th. ed. Boca Roton: CRC Press. 2005
- [181] Sohn, J. H., Pham, L. Q., Kang, H. S., Park, J. H., Lee, B. C., Kang, Y. S. (2010). Preparation of Conducting Silver Paste with Ag Nanoparticles Prepared by e-beam Irradiation. *Radiation Physics and Chemistry*. 79:1149-1153
- [182] Rejikumar, P. R., Jyothy, P. V., Mathew, S., Thomas, V., Krishnan, N. V. U. (2010). Effect of Silver Nanoparticles on the Dielectric Properties of Holmium doped Silica Glass. *Physica B*. 405: 1513–1517
- [183] Esquivel, M. R., Bohé, A. E., Pasquevich, D. M. (2001). Reactivity of a Sm₂O₃-CeO₂ Mixture with Gaseous Chlorine. *Jornadas SAM - CONAMET – AAS*. 9-16
- [184] Rami, R.M., Ravi, K.V., Veeraiah, N. and Appa, R.B. (1995). Effect of chromium impurity on dielectric relaxation effects of ZnF₂-PbO-TeO₂ glasses. *Indian Journal of Pure and Applied Physics*. 33: 48-51
- [185] Chowdari, B. V. R., Kumari, P. P. (1998). Studies on Ag₂O, M_xO_y.TeO₂ (M_xO_y = WO₃, MoO₃, P₂O₅, and B₂O₃) Ionic Conducting Glasses. *Solid State Ionics*. 113–115: 665-675
- [186] Halimah, M.K., Daud, W.M. Sidek, H.A.A., Zaidan, A.W. Zainal, A.S. (2010). Optical Properties of Ternary Tellurite Glasses. *Materials Science Poland*. 28: 173
- [187] Chanshetti, U.B., Shelke, V.A., Jadhav, S.M., Shankarwar, S.G., Chondhekar, T.K., Shankarwar, A.G., Sudarsan, V., Jogad, M.S. (2011). Density and Molar Volume Studies of Phosphate Glasses. *Physics, Chemistry and Technology*. 9: 29-36

- [188] Martin, D.M., Villegas, M.A., Gonzalo, J., Navarro, J.M.F. (2009). Characterisation of Glasses in the $\text{TeO}_2\text{-WO}_3\text{-PbO}$ system. *Journal of European Ceramic Society*. 29: 2903-2913
- [189] Mansour, E. (2012). FTIR Spectra of Pseudo-Binary Sodium Borate Glasses Containing TeO_2 . *Journal of Molecular Structure*. 1014: 1-6
- [190] Rada, S., Culea, E., Rada, M., Pascuta, P., Maties, V. (2009). Structural and Electronic Properties of Tellurite Glasses. *Journal of Materials Science*. 44: 3235-3240
- [191] Kamalaker, V., Upender, G., Prasad, M., Mouli, M. C. (2010). Infrared, ESR and Optical Absorption Studies of Cu^{2+} ions doped in $\text{TeO}_2\text{-ZnO-NaF}$ Glass System. *Indian Journal of Pure & Applied Physics*, 48: 709-715
- [192] Jha, A., Shen, S., Naftaly, M (2000). Structural Origin of Spectral Broadening of 1.5 μm Emission in Er^{3+} -doped Tellurite Glasses. *Physical Review B*. 62: 6215-6227
- [193] Burger, H., Kneipp, K., Hobert, H., Vogel, W., Kozhurkharov, V., Neov, S. (1992). Glass Formation, Properties and Structure in the $\text{TeO}_2\text{-ZnO}$ System. *Journal of Non-Crystalline Solids*. 151: 134
- [194] Wang, Y. H., Osaka, A., Miura, Y., Takada, J., Oda, K., Takahashi, K. (1988). Glass Forming Range and Properties of New Oxyhalide Glasses in the System $\text{TeO}_2\text{-PbO-PbCl}_2$. *Material Science Forum*. 32: 161-165
- [195] Kojima, S., Kodama, M. (1999). Boson Peak in Modified Borate Glasses. *Physica B*. 263-264: 336-338
- [196] Mattarelli, M., Chiappini, A., Montagna, M., Martucci, A., Ribaud, A., Guglielmi, M., Ferrari, M., Chiasera, A. (2005). Optical spectroscopy of $\text{TeO}_2\text{-GeO}_2$ glasses activated with Er^{3+} and Tm^{3+} ions. *Journal of Non-Crystalline Solids*. 351: 1759-1763
- [197] Kreibig, U., Vollmer, M. *Optical Properties of Metal Clusters*. New York: Springer Verlag. 1995
- [198] Mulvaney, P. (1996). Surface Plasmon Spectroscopy of Nanosized Metal Particles. *Langmuir*. 12: 788-800
- [199] El-Hagary, M., Emam-Ismail, M., Shaaban, E. R., Shaltout, I. (2009). Optical Properties of Glasses ($\text{TeO}_2\text{-GeO}_2\text{-K}_2\text{O}$) Thin Films co-doped with Rare Earth Oxides $\text{Sm}_2\text{O}_3/\text{Yb}_2\text{O}_3$. *Journal of Alloys and Compounds*. 485: 519-523

- [200] Reddy, B.S., Buddudu, S., Rao, K.S.R.K., Babu, P. N., Annapurna, K. (2008). Optical Analysis of Er^{3+} : Boro-Fluoro-Phosphate Glasses. *Spectroscopy Letters*. 41: 376-384
- [201] Rada, S., Pascuta, P., Rada, M., Culea, E. (2011). Effects of Samarium (III) Oxide Content on Structural Investigations of the Samarium–Vanadate–Tellurate Glasses and Glass Ceramics. *Journal of Non-Crystalline Solids*. 357: 3405-3409
- [202] Rajyasree, C., Rao, D. K. (2011). Spectroscopic Investigations on Alkali Earth Bismuth Borate Glasses doped with CuO. *Journal of Non-Crystalline Solids*. 357: 836–841
- [203] Singh, S., Singh, K. (2014). Effect of in-situ reduction of Fe^{3+} on physical, structural and optical properties of calcium sodium silicate glasses and glass ceramics. *Journal of Non-Crystalline Solids*. 386: 100–104
- [204] Castillo-Torres, J. (2013). Optical Absorption Edge Analysis for Zinc-doped Lithium Niobate. *Optics Communications*. 290: 107 – 109
- [205] Arunkumar, S., Marimuthu, K. (2013). Concentration Effect of Sm^{3+} ions in $\text{B}_2\text{O}_3\text{-PbO-Bi}_2\text{O}_3\text{-ZnO}$ Glasses – Structural and Luminescence Investigations. *Journal of Alloys and Compounds*. 565:104-114
- [206] Khafagy, A. H., El-Adawy, A. A., Higazy, A. A., El-Rabaie, S. Eid, A. S. (2008). Studies of some Mechanical and Optical Properties of $(70-x)\text{TeO}_2+15\text{B}_2\text{O}_3+15\text{P}_2\text{O}_5+x\text{Li}_2\text{O}$ Glasses. *Journal of Non-Crystalline Solids*. 354: 3152-3158
- [207] Sharma, P. and Katyal, S.C. (2008). Effect of Ge Addition on the Optical Band Gap and Refractive Index of Thermally Evaporated As_2Se_3 Thin Films. *Research Letters in Materials Science*. doi:10.1155/2008/826402
- [208] Abdel-Baki, M. and El-Diasty, F. (2011). Role of Oxygen on the Optical Properties of Borate Glass doped with ZnO. *Journal of Solid State Chemistry*. 184: 2762-2769
- [209] Dousti, M. R., Ghoshal, S. K., Amjad, R. J., Sahar, M. R., Nawaz, F., Arifin, R. (2013). Structural and Optical Study of Samarium doped Lead Zinc Phosphate Glasses. *Optics communications*. 300: 204-209
- [210] Thomas, S., George, R., Rasool, Sk. N., Rathaiah, M., Venkatramu, V., Joseph, C., Unnikrishnan, N. V. (2013). Optical properties of Sm^{3+} ions in zinc potassium fluorophosphates glasses. *Optical Materials*. 36: 242-250

- [211] Rayappan, I. A., Selvaraju, K., Marimuthu, K. (2011). Structural and Luminescence Investigations on Sm^{3+} doped Sodium Fluoroborate Glasses Containing Alkali/Alkaline Earth Metal Oxides. *Physica B*. 406: 548-555
- [212] Sanderson, R. T. (1983). Electronegativity and Bond Energy. *Journal of the American Chemical Society*. 105 (8): 2259-2261
- [213] Kesavulu, C. R., Chakradhar, R. P. S., Muralidhara, R. S., Rao, J. L. and Anavekar, R. V. (2010). EPR, Optical Absorption and Photoluminescence Properties of Cr^{3+} ions in Lithium Borophosphate Glasses. *Journal of Alloys and Compounds*. 496: 75-80
- [214] Ravikumar, R. V. S. S. N., Komatsu, R., Ikeda, K., Chandrasekhar, A. V., Reddy, B. J. (2003). EPR and Optical studies on Transition Metal doped LiRbB_4O_7 Glasses. *Journal of Physics and Chemistry of Solids*. 64: 261
- [215] Giridhar, G., Sastry, S. S., Rangacharyulu, M. (2011). Spectroscopic Studies on $\text{Pb}_3\text{O}_4\text{-ZnO-P}_2\text{O}_5$ Glasses doped with Transition Metal Ions. *Physica B*. 406: 4027
- [216] Sailaja, S., Raju, C. N., Reddy, C. A., Raju, B. D. P., Jho, Y-D., Reddy, B. S. (2013). Optical Properties of Sm^{3+} - doped Cadmium Bismuth Borate Glasses. *Journal of Molecular Structure*. 1038: 29-34
- [217] Wang, W., Zhou, S. Lei, X., Gao, H., Mao, Y. (2014). Near-infrared Quantum Cutting in $\text{Bi}^{3+}/\text{Yb}^{3+}$ co-doped Oxyfluoride Glasses via Cooperative Energy Transfer for Solar Cells. *Optical Materials*. 38: 261-264
- [218] Seshadri, M., Barbosa, L.C., Cordieiro, C.M.B., Radha, M., Sigoli, F.A., Ratnakaram, Y.C. (2015). Study of Optical Absorption, Visible Emission and NIR-Vis Luminescence Spectra of $\text{Tm}^{3+}/\text{Yb}^{3+}$, $\text{Ho}^{3+}/\text{Yb}^{3+}$ and $\text{Tm}^{3+}/\text{Ho}^{3+}/\text{Yb}^{3+}$ doped tellurite Glasses. *Journal of Luminescence*. 166: 8 - 16